Quantitative Membrane Proteomics Reveals New Cellular Targets of Viral Immune Modulators

Eric Bartee, Ashley McCormack, Klaus Früh*

Vaccine and Gene Therapy Institute, Oregon Health and Science University, Beaverton, Oregon, United States of America

Immunomodulators of pathogens frequently affect multiple cellular targets, thus preventing recognition by different immune cells. For instance, the K5 modulator of immune recognition (MIR2) from Kaposi sarcoma–associated herpesvirus prevents activation of cytotoxic T cells, natural killer cells, and natural killer T cells by downregulating major histocompatibility complex (MHC) class I molecules, the MHC-like molecule CD1, the cell adhesion molecules ICAM-1 and PECAM, and the co-stimulatory molecule B7.2. K5 belongs to a family of viral- and cellular-membrane-spanning RING ubiquitin ligases. While a limited number of transmembrane proteins have been shown to be targeted for degradation by this family, it is unknown whether additional targets exist. We now describe a quantitative proteomics approach to identify novel targets of this protein family. Using stable isotope labeling by amino acids, we compared the proteome of plasma, Golgi, and endoplasmic reticulum membranes in the presence and absence of K5. Mass spectrometric protein identification revealed four proteins that were consistently underrepresented in the plasma membrane of K5 expression cells: MHC I (as expected), bone marrow stromal antigen 2 (BST-2, CD316), activated leukocyte cell adhesion molecule (ALCAM, CD166) and Syntaxin-4. Downregulation of each of these proteins was independently confirmed by immunoblotting with specific antibodies. We further demonstrate that ALCAM is a bona fide target of both K5 and the myxomavirus homolog M153R. Upon exiting the endoplasmic reticulum, ALCAM is ubiquitinated in the presence of wild-type, but not RING-deficient or acidic motif–deficient, K5, and is targeted for lysosomal degradation via the multivesicular body pathway. Since ALCAM is the ligand for CD6, a member of the immunological synapse of T cells, its removal by viral immune modulators implies a role for CD6 in the recognition of pathogens by T cells. The unbiased global proteome analysis therefore revealed novel immunomodulatory functions of pathogen proteins.

Citation: Bartee E, McCormack A, Früh K (2006) Quantitative membrane proteomics reveals new cellular targets of viral immune modulators. PLoS Pathog 2(10): e107. DOI: 10.1371/journal.ppat.0020107

Introduction

Viral and bacterial virulence often correlates with the pathogen's ability to modulate the host's immune response. One pathway that is frequently targeted by intracellular pathogens, particularly viruses, is antigen presentation by major histocompatibility complex (MHC) class I molecules. By interfering with MHC I expression, transport, or peptide loading, viruses become invisible to cytotoxic T cells. Interestingly, many viral gene products that interfere with MHC I also target other immunologically relevant host cell proteins. For instance, US3 and US11 of human cytomegalovirus affect surface expression of both MHC I and MHC II [1,2]. The murine cytomegalovirus protein m152 causes mislocalization of both MHC I and Rae-1, an unrelated molecule that is a ligand for the activating receptor NKG2D found on natural killer cells and T cells [3,4]. Finally, the HIV-1 proteins nef and vpu both downregulate MHC I and the T cell co-receptor CD4 [5–8].

This multi-functionality is likely advantageous for the virus since it interferes with recognition by different immune cells and might counteract negative side effects of MHC I downregulation such as activation of natural killer cells. These observations, however, also raise the question of whether the currently known host cell proteins are the only targets of a given viral immune regulator or whether additional targets exist. To address this question experimentally, we selected the K5 protein of Kaposi sarcoma–associated herpesvirus (KSHV), a particularly promiscuous member of a family of viral immune modulators. KSHV encodes two homologous members of the K3 family of viral immune modulators, K5 and K3 [9,10]. These proteins display an amino-terminal RING-CH domain facing the cytoplasm followed by two membrane-traversing domains, resulting in a

Editor: Donald E. Ganem, University of California San Francisco, United States of America

Received June 16, 2006; **Accepted** September 5, 2006; **Published** October 27, 2006

DOI: 10.1371/journal.ppat.0020107

Abbreviations: ALCAM, activated leukocyte cell adhesion molecule; BST-2, bone marrow stromal antigen 2; DMVEC, dermal microvascular endothelial cell; ER, endoplasmic reticulum; GFP, green fluorescent protein; HA, hemagglutinin epitope; KSHV, Kaposi sarcoma–associated herpesvirus; MARCH, membrane-associated RING-CH; MHC, major histocompatibility complex; MS, mass spectrometry; MVB, multivesicular body; PMA, phorbol 12-myristate 13-acetate; SILAC, stable isotope labeling with amino acids in cell culture; TCR, T cell receptor; t-SNARE, target-membrane-associated soluble N-ethylmaleimide fusion protein attachment protein receptor

* To whom correspondence should be addressed. E-mail: fruehk@ohsu.edu

Synopsis

Viral immune modulators often target multiple cellular proteins for destruction. Presumably, this strategy enables viral pathogens to optimize evasion of multiple immune responses. To systematically identify such host cell targets in an unbiased fashion, Bartee et al. applied recently developed quantitative proteomics methods to identify novel targets for K5. K5 belongs to a family of viral ubiquitin ligases found in gamma-herpesviruses and poxviruses that target multiple cellular transmembrane proteins for destruction. Using stable isotope labeling combined with tandem mass spectrometry, the authors compared the abundance of proteins in membrane preparations from cells that expressed K5 to that in cells without K5. In their experiments, three novel membrane proteins (BST-2, Syntaxin-4, and ALCAM) were consistently found in lower abundance in K5-expressing cells. Importantly, the authors were able to confirm the K5-dependent downregulation of all of these proteins in independent experiments and by independent methods. ALCAM was chosen for a more in-depth analysis to firmly demonstrate that this protein is downregulated by K5 in a manner similar to other known targets. This proof-of-principle study demonstrates that novel targets of viral immune modulators can be identified with quantitative proteomics.

type III transmembrane topology [11]. K3-type immune modulators are also found in several poxviral genomes [12,13] and are most likely derived from host genes since many eukaryotic organisms, including humans, contain similar proteins, termed membrane-associated RING-CH (MARCH) proteins, or c-MIR [14,15]. Both viral and mammalian members of this family act as RING-type ubiquitin ligases (RING-E3s) and mediate the ubiquitination of lysines or cysteines in the cytoplasmic tail of transmembrane proteins [16,17]. In most cases, ubiquitination occurs post–endoplasmic reticulum (ER), and ubiquitinated transmembrane proteins are endocytosed, sorted to multivesicular bodies (MVBs), and degraded in lysosomes [9,10,12,14,18]. ER-associated proteasomal degradation has also been observed for the K3 protein of murine herpesvirus 68 [16] and for some substrates of KSHV-K5 [19].

All viral K3 family proteins studied so far, and two of the human MARCH proteins, target MHC I for degradation. Several K3 family proteins target other immunoreceptors in addition to MHC I. For example, K5 also downregulates CD1, ICAM-1, PECAM, and B7.2 [19–22], and M153R also targets CD4 [12]. While the rules for substrate selection have yet to be established, it seems evident that this protein family has evolved to target subsets of transmembrane proteins. These proteins are thus an excellent model for viral immune modulators that have more than one cellular target. In addition, these proteins are representative for other ubiquitin ligases that target certain groups of proteins, not all of which might be known [23].

K5 was initially identified by screening the KSHV genome for gene products inhibiting MHC I expression [9]. Further targets for K5 were then revealed by monitoring the expression of a small set of cell surface proteins, particularly those involved in T cell recognition of infected cells [19–21]. These experiments, however, did not rule out that expression of other cellular proteins is inhibited by K5. Ideally, to determine whether additional targets exist, the entire cell proteome would be studied in the presence or absence of K5. A method to absolutely quantify the entire protein complement of a cell has yet to be developed; however, recent advances in quantitative proteomics using stable isotope labeling allow the *relative* quantification of proteins in different samples by mass spectrometry (MS) [24].

In cell culture, the preferred method of comparative quantitative proteomics is to metabolically incorporate heavy or light forms of specific amino acids. This technique is known as stable isotope labeling with amino acids in cell culture (SILAC) [25,26]. SILAC incorporates naturally occurring amino acids (C^{12} and N^{14}) into one sample and isotopically labeled amino acids (C^{13} and N^{15}) into another sample. The ratio of the "light" to "heavy" peptide can then be determined upon MS analysis of the combined samples. SILAC has been successfully used in yeast, plant, and mammalian cells to measure relative protein abundance [27–29].

K5 is a transmembrane protein that localizes to the ER, Golgi, and plasma membranes [11,19]. Since K5 is known to degrade other transmembrane proteins, we focused on identifying proteins that were reduced upon K5 expression in ER, Golgi, and plasma membrane fractions. In three independent repeat experiments we observed that MHC I, activated leukocyte cell adhesion molecule (ALCAM), bone marrow stromal antigen 2 (BST-2), and Syntaxin-4 were consistently reduced in plasma membranes of K5-expressing cells, whereas only K5 itself was increased in any fraction. While reduced MHC I expression was expected, none of the other proteins were previously known to be affected by K5. Importantly, downregulation of each of these proteins by K5 was confirmed in independent experiments and by independent methods, thus validating the quantitative proteomics approach as a new method for identifying cellular proteins affected by viral immunomodulators.

Results

Membrane Preparation and Mass Spectrometric Analysis

Since all previously described targets of K5 were type I transmembrane glycoproteins, we hypothesized that novel targets of K5 were most likely to be found in the membrane fraction. Most targets of K5 are ubiquitinated in a post-ER compartment and then sorted to endosomes in a clathrin-dependent process [30]. We recently showed, however, that newly synthesized CD31/PECAM is degraded by K5 prior to ER exit by ER-associated proteasomal degradation [19]. It is thus conceivable that novel targets could be eliminated from either the plasma membrane or from intracellular membranes, particularly within the exocytic pathway. For these reasons, we wanted to measure changes in the proteome of the plasma membrane, the Golgi membrane, and the ER membrane.

To measure changes in the membrane proteome we used stable-isotope-labeled amino acids coupled with mass spectrometric analysis. Since isotope labeling incorporates differentially weighted tags directly into proteins, this method allows the fractionation of membranes after combination of samples, thus minimizing variation due to sample preparation. The weight differential is then used to discriminate between peptides derived from each sample and to determine relative protein abundance by mass spectrometric analysis. Previous work has demonstrated that isotopically labeled amino acid analogs are indistinguishable from the natural product with respect to supporting cell growth in tissue

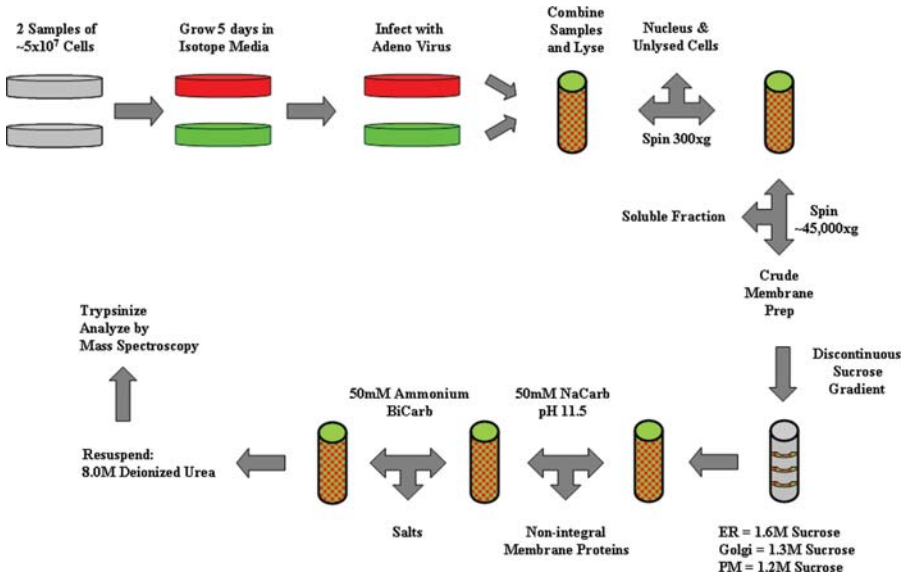

Figure 1. Schematic Representation of the SILAC Labeling and Purification Protocol

HeLa cells were grown for 5 d in labeling medium to ensure complete labeling. They were then infected with either adenovirus vector (light sample) or adenovirus-expressing K5 (heavy sample). Then 24 h post-infection, cells were harvested and counted, and equal numbers of cells combined. Samples were lysed in a Dounce homogenizer and unlysed cells removed by centrifugation. Membrane and soluble proteins were separated by centrifugation. The membrane pellet was resuspended, and different membrane fractions were separated over a discontinuous sucrose gradient. The bands corresponding to the plasma membrane (PM), Golgi, and ER fractions were removed and the proteins pelleted. The resulting pellet was then washed with sodium carbonate to remove non-integral membrane proteins, followed by ammonium bicarbonate to remove salts and other impurities. The final pellet was resuspended in 8 M urea and digested with trypsin for MS/MS analysis.

DOI: 10.1371/journal.ppat.0020107.g001

culture [25]. For our experiments, we added both $N^{15}/_{6}C^{13}$-labeled leucine and $_{2}N^{15}/_{6}C^{13}$-labeled lysine to HeLa cells. Since trypsin cleaves after lysines, and almost 70% of predicted tryptic peptides in the human genome contain at least one leucine, this double labeling procedure ensures that most tryptic peptides will contain at least one isotopic amino acid [26]. HeLa cells were grown in labeling medium for 5 d prior to expression of K5 via adenovirus transduction. Due to rapid doubling of HeLa cells, this time frame allowed for the complete incorporation of isotopic amino acids (unpublished data). Control cells were grown in medium containing natural amino acids and transduced with the same multiplicity of infection of control adenovirus. K5-mediated downregulation of MHC I was confirmed by flow cytometry 24 h post-infection (unpublished data). To minimize variation due to biochemical procedures, plasma membrane, ER, and Golgi fractions were generated by sucrose gradient separation after lysis of the combined labeled and unlabeled cells (Figure 1). To further control for technical and biological variation, we repeated each experiment three times. Tryptic peptides from the resulting fractions were separated by two sequential chromatography steps (strong cation and reverse phase) prior to analysis by MS using an LCQ ion-trap instrument in data-dependent MS/MS mode. Tandem mass spectra of dissociated peptides were used to search the human subset of the UniProt database, which was spiked with the viral K5 sequence using SEQUEST [31]. To discriminate true assignments of MS/MS spectra to peptide sequences from false assignments, we applied PeptideProphet software using a score of 0.85 as the cutoff value for each identified peptide [32].

For each fraction we identified 500–700 unique proteins by at least one peptide in at least one experiment (Figure 2A). Of these, 100–150 proteins were identified in all three experiments, a finding that is consistent with previous reports [33]. To validate the membrane preparations, we analyzed proteins that were identified in all three replicate experiments of each fraction with respect to their subcellular localization (Figure 2B). The plasma membrane fraction contained a large percentage of predicted cell surface proteins. The ER and the Golgi fraction contained both bona fide ER- and Golgi-resident proteins and many plasma membrane or transmembrane proteins, presumably en route to the cell surface. In addition, all fractions contained significant numbers of proteins predicted to localize to other intracellular organelles such as the nucleus, cytoplasm, or mitochondria. These proteins are likely derived from contaminating protein fractions. Since K5 is not expected to affect proteins in these compartments, these proteins serve as internal controls.

Differentially Expressed Proteins

To identify proteins whose expression was altered by K5, we analyzed proteins identified in all three experiments using the program ASAPRatio [34]. ASAPRatio calculates expression ratios based on peak intensities such as those shown in Figure 2C. Since a 1.5-fold cutoff was previously shown to reflect a significantly different protein level [26], we considered proteins differentially expressed if they displayed higher than a 1.5-fold change in either direction. However, instead of limiting our analysis to proteins identified by multiple peptides in a single experiment as done previously [26], we accounted for biological variation by focusing on proteins that changed in the same direction in all three experiments, regardless of the number of peptides identified in either experiment. Using these criteria, only one protein changed in the ER and Golgi fractions. This protein was K5 itself, which was scored as

A

	PM	Golgi	ER
Proteins in Any Experiment	570	637	666
Proteins in All Experiments	109	140	132
Proteins Changing > 1.5 Fold in 2 of 3 Experiments	28	23	13
Proteins Changing > 1.5 Fold in 3 of 3 Experiments	5	1	1

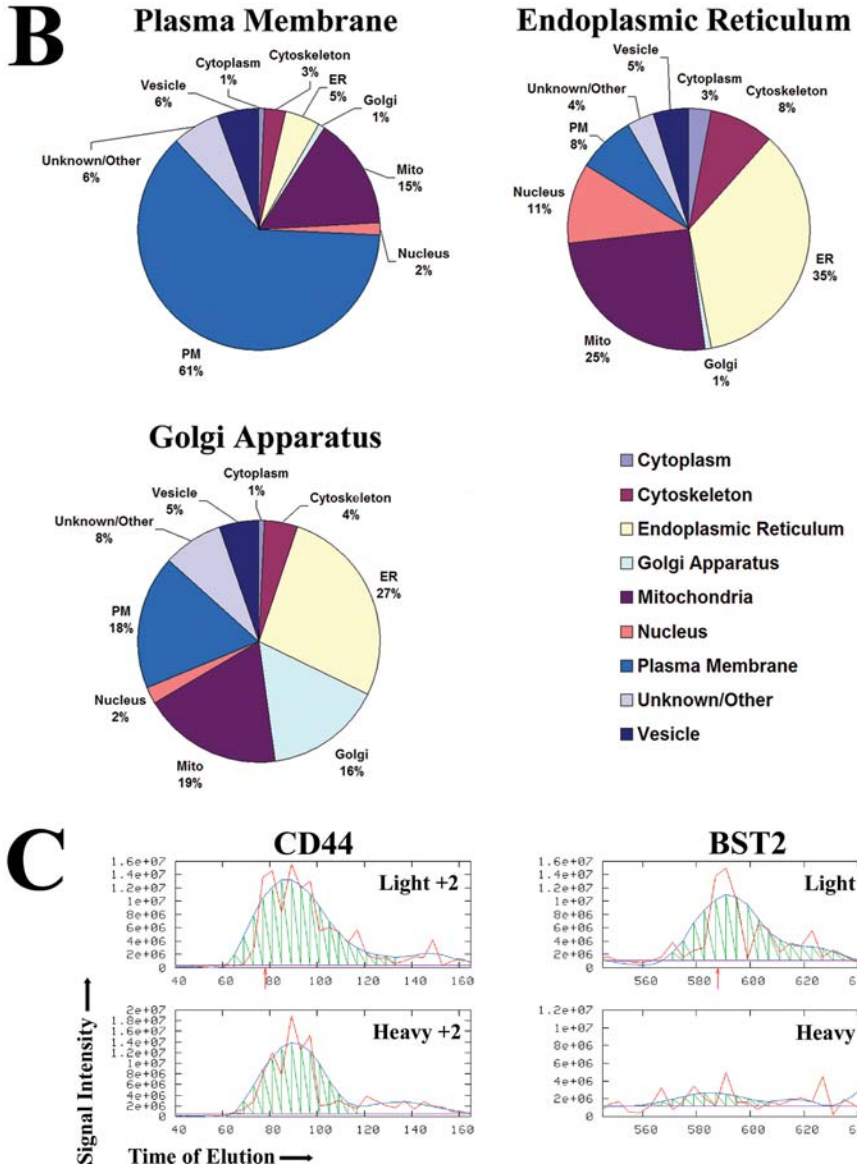

Figure 2. Protein Identification and Differential Peptide Quantification

(A) Approximately 500–700 proteins were identified by at least one peptide in each fraction; however, fewer than 150 proteins per fraction were identified in all three replicates. Of these, only five proteins changed more than 1.5-fold in the plasma membrane (PM) fraction, while only one protein changed more than 1.5-fold in all three replicates of either the Golgi or ER fractions.

(B) Proteins present in all three replicates of each fraction were analyzed for their predicted subcellular distribution using annotations in the Swiss-Prot proteomics database.

(C) Comparison of signal intensities obtained for selected peptides from the indicated proteins. The red line indicates the actual raw data recovered from the mass spectrometer; the blue line is a hypothetical best fit line drawn to help analyze elution time of the light and heavy peptides. The orange arrows indicate the time at which the initial MS/MS scan was initiated. Peptides derived from unaffected proteins, such as CD44, display a similar intensity for both the light and heavy isotopes. Peptides derived from differentially expressed proteins, such as BST-2, show clearly different intensity peaks for the light and heavy peptides. Note the slightly different scale for intensity of each peptide.

DOI: 10.1371/journal.ppat.0020107.g002

"upregulated" since it was present only in the transduced samples. K5 was also scored as upregulated in the plasma membrane fraction of K5-expressing cells. Additionally, four proteins were downregulated in all three plasma membrane samples (Figure 2A; Table 1). Among this list were peptides mapping to the *HLA-A01* allele, which were present in significantly lower amounts in the plasma membrane fraction, but not in the ER or Golgi fractions. The lack of statistically significant MHC I downregulation in the ER fraction is consistent with the observation that MHC I assembly in the ER is not affected by K5 [9,10]. Since both internal controls—transduced K5 as well as the K5 target protein MHC I—were successfully identified as displaying altered ratios, we anticipated that the three remaining proteins in the plasma membrane fraction had a high chance of being true positive results.

Each of these three proteins was not previously identified as downregulated by K5: BST-2 (also known as HM1.24 and CD316), Syntaxin-4, and ALCAM (CD166). To independently confirm the downregulation of these proteins, we obtained specific antibodies for each and analyzed their expression in the presence or absence of K5.

BST-2

BST-2 (Hs.118110) is a protein of largely unknown function that has been implicated in normal as well as malignant B cell differentiation [35,36]. BST-2 displays a very unusual topology in that it contains both an amino-terminal transmembrane domain and a carboxy-terminal GPI linker [37]. Despite this topological difference and lack of relationship to other K5 targets, BST-2 was consistently scored as the most strongly underrepresented protein in K5-expressing cells (Table 1). A dramatic reduction of BST-2 expression was confirmed in immunoblot of Ad-K5-infected HeLa cells, whereas BST-2 was unaffected in Mock- or Ad-WT-infected cells (Figure 3A). BST-2 expression was also strongly reduced upon adenovirus-mediated expression of the human K5 homolog MARCH-VIII, but was less affected by the HIV protein vpu, which recruits a cellular ubiquitin ligase. To determine whether downregulation of BST-2 required the ubiquitin ligase activity of K5, we transfected a catalytically inactive mutant of K5 (K5-RING) that lacks two critical cysteines in the K5-RING domain [38], and monitored BST-2 expression by immunoblot. While transiently transfected K5 was still able to downregulate BST-2, the K5-RING construct

Table 1. SILAC Analysis Yields Three Proteins Displaying Reproducibly Altered Protein Ratios

Category	Protein	Protein Ratio ± Standard Deviation			Unique Peptides
		Experiment 1	Experiment 2	Experiment 3	
Plasma membrane fraction	ALCAM	2.04 ± 0.24	2.59 ± 0.96	1.68 ± 0.19	(1) WKYEKPDGSPVFIAFR
		(1, 2)	(1, 3, 4)	(1)	(2) ALFLETEQLKK
					(3) DLGNMEENKK
					(4) WSLTLIVEGKPQIK
					(5) SMIASTAITVHYLDLSLNPSGEVTR
	BST-2	3.14 ± 0.36	3.19 ± 2.39	1.83 ± 0.59	(1) ENQVLSVR
		(1, 2, 3)	(2, 3)	(2)	(2) KVEELEGEITTLNHK
					(3) LQDASAEVER
	Syntaxin-4	1.55 ± 2.9	2.20 ± 0.87	1.67 ± 0.31	(1) AIEPQKEEADENYNSVNTR
		(1, 2)	(3, 4)	(4)	(2) VALVVHPGTAR
					(3) KTQHGVLSQQFVELINK
					(4) TQHGVLSQQFVELINK
	MHC I	2.69 ± 0.89	2.60 ± 2.52	1.68 ± 0.22	(1) DGEDQTELVETRPAGDGTHQK
		(1, 2, 3, 4, 5)	(1, 2, 3, 4, 7, 8, 9, 10, 11, 12)	(1, 3, 5, 8)	(2) RYLENGKETLQR
					(3) YLENGKETLQR
					(4) AQSQTDRVDLGTLR
					(5) YTCHVQHEGLPEPLTLR
					(6) YTCHVQHEGLPK
					(7) GYHQYAYDGK
					(8) GYHQYAYDGKDYIALK
					(9) KGGSYSQAASSDSAQGSDVSLTACK
					(10) THMTHHAVSDHEATLR
					(11) HKWEAAHVAEQWR
					(12) THVTHHPVSDHEATLR
	KSHV-K5	0.00 ± 0.00	0.26 ± 0.05	0.30 ± 0.19	(1) ALYAANNTR
		(1)	(1, 2, 3, 4)	(3)	(2) EEVGNEGIHPCACTGELDNNHPQCLSTWLTVSR
					(3) TDLCAPTKKPVR
					(4) VTVLPYR
ER fraction	KSHV-K5	0.29 ± 0.02	0.04 ± 0.01	0.06 ± 0.06	(1) ALYAANNTR
		(1, 2)	(1, 2)	(2, 3, 4)	(2) EEVGNEGIHPCACTGELDNNHPQCLSTWLTVSR
					(3) TDLCAPTKKPVR
					(4) VTVLPYR
Golgi fraction	KSHV-K5	0.20 ± 0.10	0.02 ± 0.01	0.10 ± 0.11	(1) ALYAANNTR
		(1, 4)	(1, 2)	(1, 2, 3, 4)	(2) EEVGNEGIHPCACTGELDNNHPQCLSTWLTVSR
					(3) TDLCAPTKKPVR
					(4) VTVLPYR

DOI: 10.1371/journal.ppat.0020107.t001

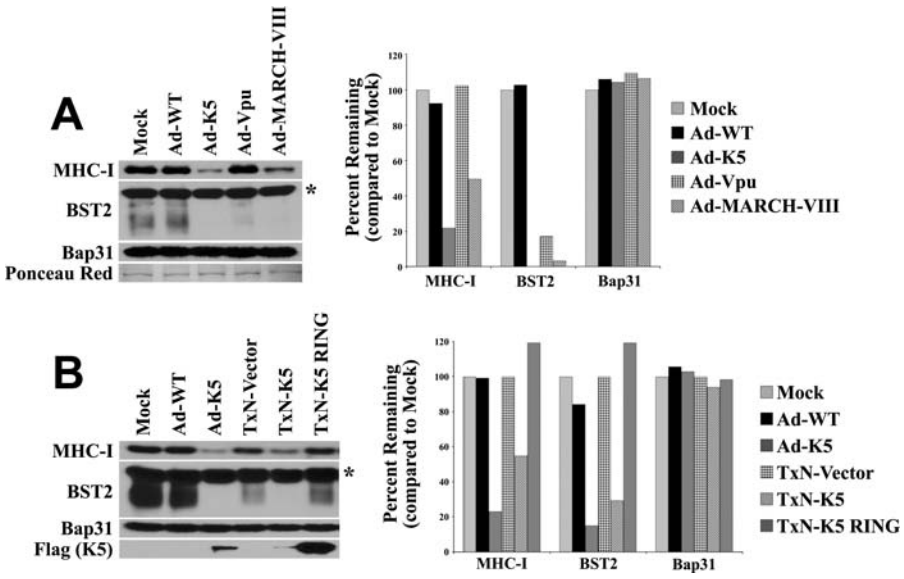

Figure 3. BST-2 Is Differentially Expressed in K5-Expressing Cells

HeLa cells were transduced with Ad-WT, Ad-K5, Ad-vpu, or Ad-MARCH-VIII. Then 24 h post-infection, cells were harvested and whole cell lysates were analyzed for the abundance of BST-2 and MHC I by Western blotting. Note that BST-2 is highly glycosylated and runs as multiple bands. The high molecular weight band marked with an asterisk is non-specific. Equal protein loading was confirmed by visualizing the ER resident chaperone Bap31 as well as general protein staining with Ponceau red ([A], left). The intensity of each band was quantified using densitometry ([A], right). The specificity of BST-2 downregulation was confirmed by transfecting K5 or a catalytically inactive K5-RING mutant, which showed no effect on either MHC I or BST-2 (B). The protein bands corresponding to BST-2 are more intense in (B) than in (A) because of longer exposure of the autoradiograph as well as variation in electrophoretic separation. Note that the same lysates were analyzed in lanes 1–3 of the blots in both (A) and (B).

DOI: 10.1371/journal.ppat.0020107.g003

showed no effect despite significantly higher levels of expression (Figure 3B). Whether this reduction of BST-2 levels is a direct consequence of K5 ubiquitinating BST-2, or an indirect consequence of the downregulation of other proteins by K5, has not yet been established. However, these experiments clearly confirm that BST-2 protein levels are reduced in K5-expressing cells and demonstrate that this reduction requires catalytically active K5.

Syntaxin-4

The second protein identified as downregulated by K5 was Syntaxin-4 (Hs.83734). Syntaxins belong to the target-membrane-associated soluble N-ethylmaleimide fusion protein attachment protein receptor (t-SNARE) family and are responsible for correctly targeting and fusing intracellular vesicles during transport [39]. Syntaxin-4 is a plasma membrane–localized t-SNARE and mediates docking of transport vesicles at the cell surface. Interestingly, Syntaxin-6, a Golgi-localized t-SNARE, was previously observed to associate with MARCH-II and MARCH-III, human homologs of K5 [40,41]. To confirm the reduction of Syntaxin-4 protein in K5-expressing cells and to determine whether K5 or any of the MARCH proteins associate with Syntaxin-4, we performed immunoblots and immunofluorescence experiments. Reduced levels of Syntaxin-4 were observed in K5-expressing HeLa cells, thus confirming the mass spectrometric results (Figure 4A). Interestingly, Syntaxin-4 levels were also reduced upon expression of MARCH-VIII, but not upon expression of vpu, suggesting that Syntaxin-4 is specifically targeted by transmembrane RING-CH proteins. In immune fluorescence analysis of control cells, Syntaxin-4 was observed at the plasma membrane. Expression of K5 led to a decrease in the overall intensity of Syntaxin-4, but there was no obvious co-localization (Figure 4B). In contrast, significant co-localization was observed upon transfection of all MARCH proteins, except for MARCH-III and a naturally occurring truncated splicing product to MARCH-IX ("–RING" in Figure 4B) [14]. Moreover, Syntaxin-4 seemed to be enriched in the subcellular compartments corresponding to the subcellular localization previously shown for the MARCH proteins [14]. Thus, MARCH-IV and MARCH-VIII relocated Syntaxin-4 to the Golgi and endosomes, respectively. Since these results are similar to the previously reported binding of Syntaxin-6 to MARCH-II and MARCH-III [40,41], it seems highly likely that Syntaxin-4 also interacts with the MARCH proteins with which it co-localizes.

The lack of co-localization of Syntaxin-4 with K5 could be due to K5 degrading Syntaxin-4. However, Syntaxin-4 levels are also reduced in MARCH-VIII-expressing cells, yet MARCH-VIII clearly associates with Syntaxin-4. Alternatively, it could be that only the minor fraction of K5 that traffics to the plasma membrane [19] interacts with Syntaxin-4, whereas the major, ER-localized population of K5 molecules is unable to do so. To determine whether ER exit was the determining factor for co-localization with Syntaxin-4, we generated truncated versions of MARCH proteins that were unable to leave the ER. Previous work has demonstrated that a carboxy-terminal PDZ motif in MARCH proteins is required for their forward transport since deletion of the final four amino acids resulted in ER retention of MARCH-II and MARCH-III [40,41]. While we could not confirm such a role for the carboxy-terminal 45 amino acids in MARCH-VIII, we did observe that MARCH-VIII truncated by 62 or 74 amino acids was unable to exit the ER (Figure 4C). Importantly, ER-resident MARCH-VIII mutants did not interact with Syntaxin-4. This raised the possibility that Syntaxin-4 regulates ER

exit of MARCH-VIII by binding within the 16 residues that differ between the Δ46 and Δ62 mutants. Small interfering RNA knockdown of Syntaxin-4, however, had no effect on MARCH-VIII localization (unpublished data), so we consider this hypothesis unlikely. Therefore, we conclude that Syntaxin-4 associates only with MARCH proteins that have left the ER. These data also render it highly likely that Syntaxin-4 associates, at least transiently, with the minor fraction of surface-expressed K5. This K5 fraction is not visible by immune fluorescence analysis, but can be detected by cell surface biotinylation [19]. Our data further suggest that K5 and MARCH proteins not only interact with, but also degrade syntaxins. Since syntaxins play a major role in vesicular traffic, the reduction of syntaxin levels could mislocalize transmembrane proteins, which might facilitate their targeting for ubiquitination. Further work will be required to address the role of syntaxins in the function of this protein family.

ALCAM (CD166)

ALCAM (CD166, Hs.591293) is a type I transmembrane glycoprotein of the Ig superfamily that is the ligand for the scavenger receptor CD6 on T cells [42]. The ALCAM–CD6 interaction is part of the immunological synapse and is considered a co-stimulatory signal involved in lymphocyte activation and thymocyte development [43–45]. Using transfection of a hemagglutinin epitope (HA)–tagged construct, we confirmed that K5 very efficiently eliminated ALCAM-HA upon co-transfection (Figure 5A). Additionally, downregulation of ALCAM from the cell surface was confirmed by flow cytometry of HeLa cells transduced with Ad-K5. In contrast to ALCAM, K5 did not alter surface expression of CD9 or CD29 (Figure 5B). The co-stimulatory function of ALCAM renders this molecule an attractive target for viral immune modulators. To determine whether other viral K3 family proteins target ALCAM, we transfected KSHV-K3 and the myxomavirus homolog M153R and monitored ALCAM expression by flow cytometry. Interestingly, M153R clearly reduced ALCAM surface levels, whereas the K3 protein, the most closely related K5 homolog, did not affect ALCAM (Figure 5C). This result is consistent with previous observations that K3 targets are limited to classical and nonclassical MHC I–like molecules [9,10,20], whereas both K5 and M153 display broader substrate specificity [12,21,22]. Within the MARCH family, MARCH-IV and MARCH-IX downregulated ALCAM to a significant degree, while a modest effect was observed with MARCH-VIII (Figure 5C). The RING and transmembrane domains of MARCH-IV and MARCH-IX are highly homologous to each other, and this result is consistent with previous observations showing that the range of substrates for these two MARCH proteins overlaps with that of K5 [14].

The catalytically inactive K5-RING construct [38], as well as a K5 construct lacking acidic clusters in its carboxy-terminal domain (K5DE12) [19,46], did not affect surface expression of ALCAM (Figure 5C). These data suggest that downregulation of ALCAM requires the ubiquitin ligase activity and proper subcellular targeting of K5.

To investigate whether ALCAM downregulation occurs in KSHV-infected endothelial cells, we took advantage of the fact that K5 is not expressed in latently infected dermal microvascular endothelial cells (DMVECs), but can be induced upon addition of phorbol 12-myristate 13-acetate (PMA), which activates the lytic cycle [19]. As shown previously, PMA treatment reduced expression of MHC I on the cell surface of KSHV-infected DMVECs, but not uninfected DMVECs (Figure 5D). The mean florescence of ALCAM was unchanged in latently infected DMVECs, but was reduced approximately 2-fold upon PMA treatment. In contrast, levels of CD81, a multiple transmembrane-spanning plasma membrane protein that is elevated in latently infected cells, did not change upon PMA treatment. Since PMA treatment does not induce lytic gene expression, and hence K5 expression, in all of the KSHV-infected cells [47], the actual levels of downregulation of both MHC I and ALCAM might be considerably higher in individual cells. The correlation of ALCAM downregulation and K5 expression, however, renders it highly likely that virally expressed K5 is causing this effect.

Taken together, these data suggested that ALCAM is a bona fide substrate for the viral ubiquitin ligase K5. To confirm that ALCAM downregulation involved K5-dependent conjugation of ubiquitin, we transfected HeLa cells with ALCAM-HA either in the presence or absence of Ad-K5. Ad-vpu, Ad-K5DE12, and Ad-MARCH-VIII were used as controls. Then, 24 h post-transfection, cells were lysed and ALCAM precipitated using an antibody against the HA epitope. Samples were resolved on a SDS-PAGE gel, and the presence of ubiquitinated ALCAM-HA was analyzed by immunoblotting with the anti-ubiquitin antibody P4D1. In cells transfected with ALCAM-HA alone, ubiquitinated ALCAM-HA was undetectable (Figure 6A). In the presence of K5, however, substantially increased levels of ubiquitinated ALCAM-HA were observed, consistent with K5-mediated ubiquitination of ALCAM. Acidic motif–deleted K5 and HIV-vpu had no effect, whereas MARCH-VIII slightly increased ALCAM-HA ubiquitination, consistent with the slight downregulation of endogenous ALCAM observed by flow cytometry.

Depending on the subcellular localization of the ubiquitination reaction, K5 targets are degraded in lysosomes or by the proteasome [19]. To determine which degradation system was responsible for ALCAM degradation, we followed the maturation and degradation of ALCAM-HA using pulse-chase analysis in the presence of proteasomal inhibitors or inhibitors of endosomal acidification. In the absence of K5, ALCAM-HA acquired complete resistance to endoglycosidase H within 2 h post-labeling, indicating its intracellular transport through the Golgi complex (Figure 6B). After chasing for 8 h, ALCAM-HA levels remained high in control cells, showing only a minor reduction due to endogenous turnover. Expression of K5 did not alter ALCAM biosynthesis or trafficking through the Golgi; however, amounts of endoglycosidase H–resistant ALCAM were significantly reduced, consistent with a post-Golgi degradation mechanism. K5-dependent degradation of ALCAM was inhibited by inhibiting lysosomal acidification with concanamycin A but not by the proteasomal inhibitor MG132. A similar effect was seen with fluorescent microscopy analysis (unpublished data). To determine whether ALCAM is targeted to lysosomes via the MVB pathway, we co-transfected K5 with a dominant negative version of the AAA-ATPase Vps4 (Vps4mut), which prevents MVB formation [48]. Expression of dominant negative Vps4 partially restored surface expression of both MHC I and ALCAM measured using flow cytometry, whereas

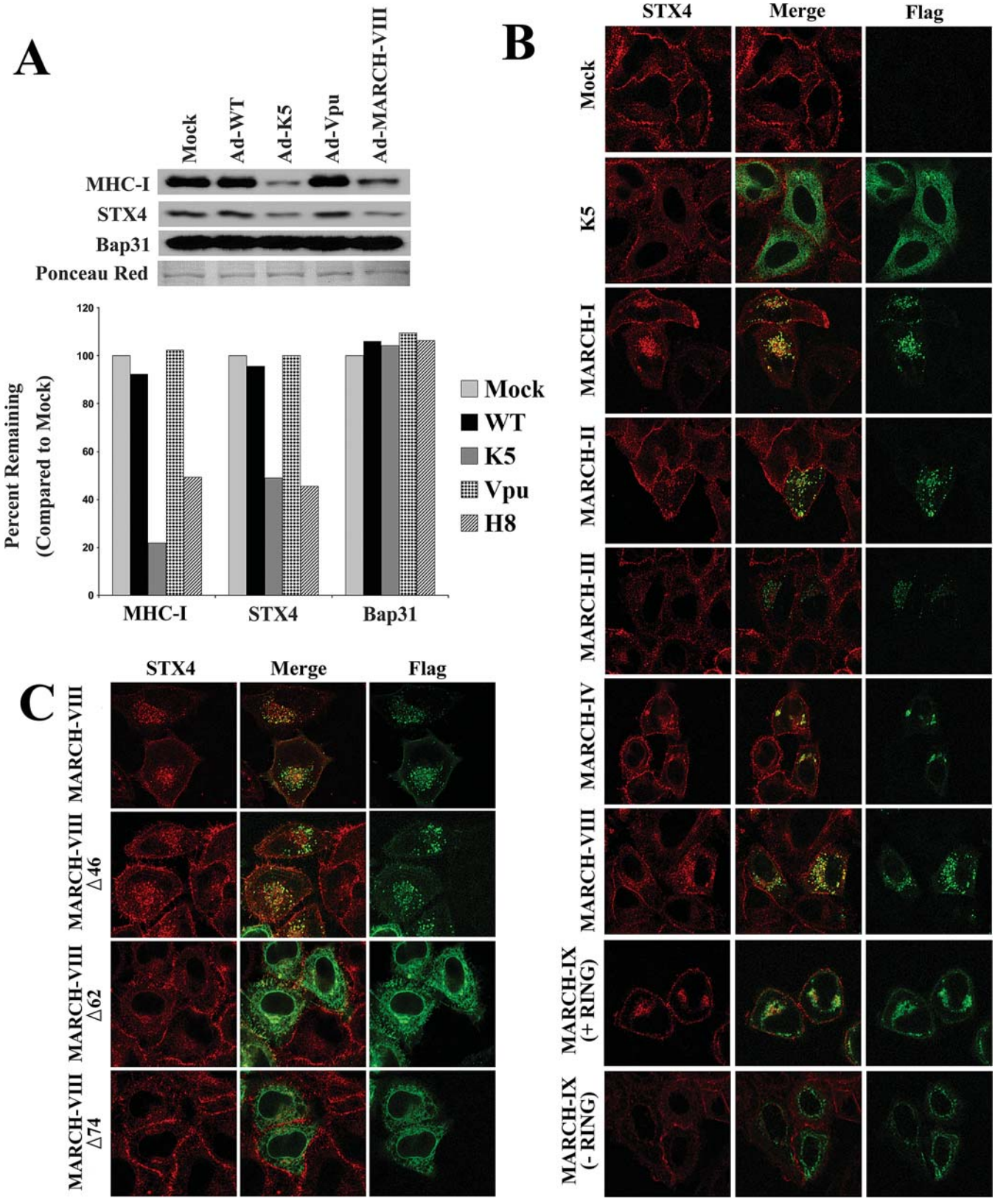

Figure 4. K5 Causes Downregulation but Not Relocalization of Syntaxin-4

(A) HeLa cells were transduced with Ad-WT, Ad-K5, Ad-vpu, or Ad-MARCH-VIII. Then 24 h post-infection, cells were harvested and whole cell lysates were analyzed as in Figure 3, except that antibodies specific for Syntaxin-4 were used. Expression of K5 resulted in a moderate but reproducible reduction of Syntaxin-4 levels.

(B) To determine if K5 or MARCH proteins caused a relocalization of Syntaxin-4, HeLa cells were transfected with C-terminally FLAG-tagged versions of the E3 enzymes shown. Cells were then analyzed for the location of Syntaxin-4 (using an Alexa Fluor 594–conjugated secondary antibody, shown as red)

as well as the overexpressed E3 (using a FITC-conjugated anti-FLAG antibody, shown as green). Co-localization of Syntaxin-4 and the ubiquitin ligases is revealed as yellow co-staining. While K5 did not co-localize with Syntaxin-4, several MARCH family proteins relocalized Syntaxin-4 to a MARCH-containing compartment. A naturally occurring splice variant of MARCH-IX that lacks a complete RING domain and fails to exit the ER was unable to relocalize Syntaxin-4.
(C) C-terminal truncation mutants of MARCH-VIII that failed to exit the ER do not co-localize with Syntaxin-4.
DOI: 10.1371/journal.ppat.0020107.g004

wild-type Vps4 had only a minor effect (Figure 6C). Taken together, these data indicate that K5 ubiquitinates ALCAM in a post-ER compartment, thus triggering ubiquitin-mediated endocytosis and targeting of ALCAM for lysosomal destruction via the MVB pathway. Since this mechanism is similar to that of other K5 targets, we conclude that ALCAM is a novel substrate for K5 as well as a target for M153R. Thus, we present a novel approach for the systematic identification of substrates for transmembrane ubiquitin ligases as well as viral immune modulators targeting membrane proteins.

Discussion

The goal of this work was to systematically search for novel targets of viral immune modulators. To this end, we applied SILAC, a quantitative proteomics method based on metabolic isotope labeling. Until now, the SILAC method was mainly used for global comparative proteomics experiments expected to yield a relatively large number of changes, such as the comparison of cell surface proteins from T helper 1 versus T helper 2 cells [49], differential protein secretion from cancer versus normal cells [50], proteins associated with stimulation of a given receptor [51], or changes in substrates trapped by a mutant protease complex upon stress activation [52]. To our knowledge, however, this is the first time SILAC has been used in an experiment where only a few protein changes were expected. A major challenge for this approach was to identify true changes among the high rate of false positives that are caused by false peptide identification, inaccurate measurements of peptide intensity, or biological variation arising during the labeling procedure. For these reasons, protein quantitation in SILAC experiments is usually limited to proteins that are identified by two or more peptides (e.g., [52]). This allows confirmation of each peptide by a second peptide from the same protein, thus raising confidence that calculated protein ratios are accurate. This approach, however, severely limits proteome coverage, particularly for low abundance proteins that are often identified by only one peptide. For this reason we sought to include all identified proteins in our analysis regardless of how many peptides were used in their identification. Inclusion of single peptide identifications raised the background for individual experiments to the point that it was impossible to discriminate between true positives and false positives purely by a fold-change cutoff (unpublished data). By analyzing three biological replicate experiments, we were able to identify true positives. The use of three replicates sets a high threshold and might exclude potential substrates. However, upon lowering the stringency (either two out of three experiments or several peptides in one experiment), we were unable to confirm additional targets from a few selected candidates, suggesting a dramatic increase in the false positive rate (unpublished data). In contrast, using three replicates resulted in 100% specificity.

The rate of false negatives—the proteins that were affected by K5 but were eliminated by these selection criteria—is difficult to gauge since only a few of the known K5 targets (MHC I and ICAM-1) are present in HeLa cells. No peptides derived from ICAM-1 were ever identified, probably since ICAM-1 is expressed at low levels in this cell type unless induced by pro-inflammatory stimuli. A better estimate of the false negative rate could potentially be obtained by analyzing other cell types, such as B cells and endothelial cells that express high levels of multiple K5 targets. The sensitivity of the method is therefore presently unknown. However, since only a fraction of the membrane proteome was identified here, it is likely that additional targets for K5 will be revealed by improved protein identification, improved analysis methods, or improved enrichment of the target proteome.

Using specific antibodies as well as epitope tagging, we confirmed the K5-dependent reduction in protein abundance for BST-2, Syntaxin-4, and ALCAM in independent experiments. Of these proteins, only BST-2 was unrelated to protein families previously shown to interact with or be targeted by the MARCH family or K3 family proteins. Downregulation of BST-2 required the ubiquitin ligase function of K5, suggesting that the reduced expression of BST-2 is linked to the enzymatic function of K5. However, we have not ruled out the possibility that BST-2 levels are indirectly affected by another protein that is targeted by K5. Thus, one of the limitations of the SILAC approach is that it does not discriminate between proteins that are targeted directly and those that are targeted indirectly by the transmembrane ubiquitin ligases. This limitation could possibly be overcome by combining the SILAC analysis with proteomic analysis of ubiquitinated proteins [53,54]. Further experiments will be needed to determine whether BST-2 is a bona fide target of K5 or related molecules. If so, it could be that BST-2 plays an as yet unknown role in immune defense.

The identification of Syntaxin-4 by the SILAC method was surprising for several reasons. First, the K5-induced changes in Syntaxin-4 levels were relatively modest compared to those for MHC I, ALCAM, or BST-2. This demonstrates that even moderately changing proteins can be identified by SILAC, provided these changes can be measured reproducibly. Second, previous observations with MARCH proteins indicated that syntaxins interact with this protein family, but evidence for degradation was not reported. Third, Syntaxin-4 is quite different from the typical K5 substrates, which mostly represent type I glycoproteins of the Ig superfamily. In contrast, Syntaxin-4 is a type II transmembrane protein with a carboxy-terminal tail-anchor and multiple coiled-coil domains. As discussed above for BST-2, it might therefore be that K5 mediates degradation of Syntaxin-4 through an indirect mechanism. However, the co-localization of Syntaxin-4 with all MARCH proteins that locate to post-ER compartments renders it likely that Syntaxin-4 interaction is a general feature of the entire protein family, including K5. Syntaxin-4 thus joins a

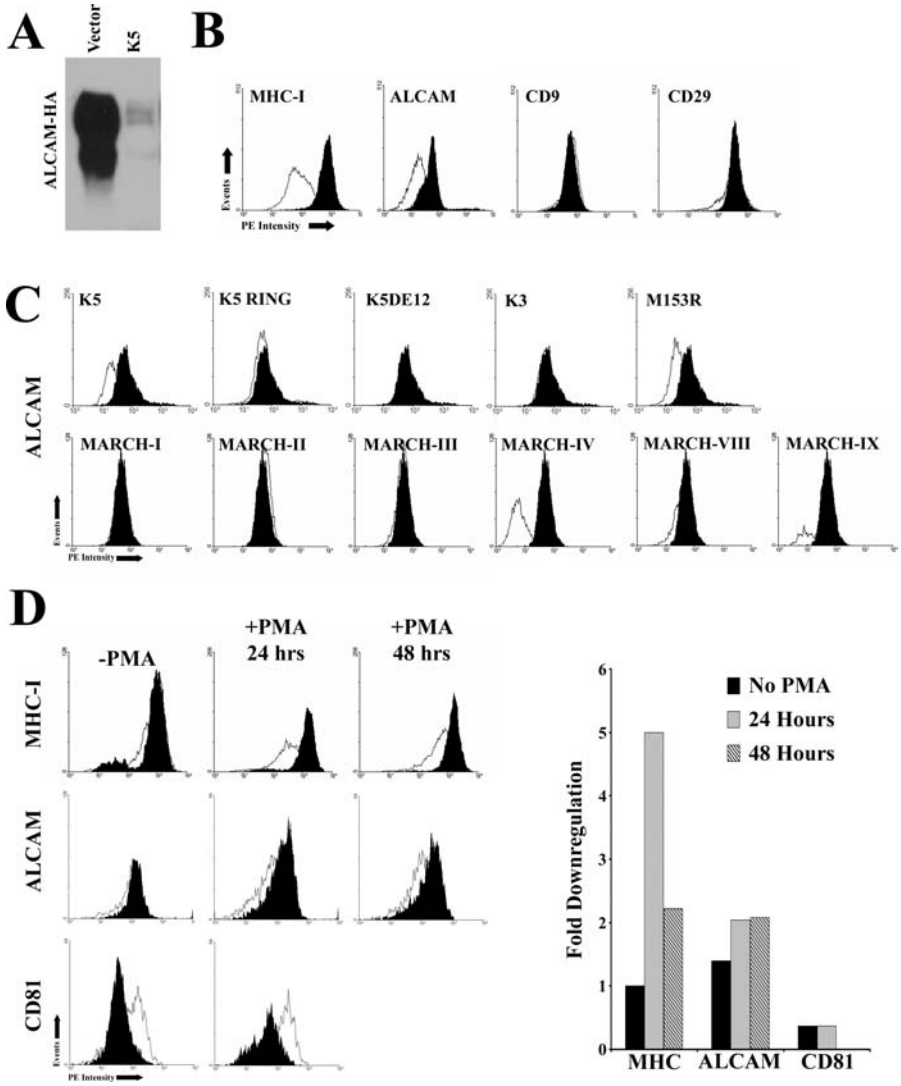

Figure 5. K5 Downregulates ALCAM

(A) C-terminally HA-tagged ALCAM was co-transfected with K5 or control plasmid. Then 24 h post-transfection, cells were harvested and the abundance of ALCAM-HA in each lysate was measured by Western blotting with anti-HA antibody.

(B) Cell surface expression of endogenous ALCAM in the presence or absence of K5 was determined by flow cytometry. HeLa cells were co-transfected with K5 and a green fluorescent protein (GFP)–expressing plasmid to identify transfectants. Then 24 h post-transfection, cells were harvested and stained with antibodies against MHC I, ALCAM, CD9, and CD29. Both vector (solid black) and K5-transfected (white) cells were gated for GFP-expressing cells.

(C) ALCAM downregulation by K5-related proteins was determined by transfecting HeLa cells with viral K3 family members (K3 and M153R) and the indicated human MARCH proteins. Also examined were mutant K5 proteins with enzymatically inactive RING-CH domains (K5-RING) or lacking acidic residues implicated in subcellular targeting (K5DE12). Neither K5 mutant reduced ALCAM levels. KSHV K3 was unable to downregulate ALCAM, whereas the myxomavirus M153R protein significantly reduced ALCAM surface expression. Two of the MARCH proteins, MARCH-IV and MARCH-IX, strongly downregulated ALCAM, while MARCH-VIII showed a minimal effect.

(D) To determine whether ALCAM expression was affected by KSHV, latently infected immortalized DMVECs were treated with PMA to induce expression of lytic genes including K5. Surface levels of either MHC I or ALCAM were measured by flow cytometry 24 and 48 h post-induction. CD81, measured at 24 h, was used as a control. The ratio between the mean fluorescence intensity of infected and uninfected samples from these experiments is shown as fold change on the right.

DOI: 10.1371/journal.ppat.0020107.g005

growing list of vesicular trafficking regulators interacting with MARCH family or K3 family proteins. In addition to the above-mentioned Golgi t-SNARE Syntaxin-6 that interacts with MARCH-II and MARCH-III, this list includes the COP-I adaptor protein PACS-2 [19] and the ER/*cis*-Golgi-located adaptor protein Vap-A (R. Means and S. Lang, personal communication). Either such interactions could locate the RING-CH proteins to specific vesicular compartments, or the RING-CH protein could interfere with the function of the vesicular regulators. In the case of Syntaxin-4, it is conceivable that downregulation of Syntaxin-4 reduces the exocytosis of certain proteins. For instance, Syntaxin-4 is required for the secretion of insulin in pancreatic beta cells [55]. One could therefore speculate that, by degrading Syntaxin-4, KSHV prevents the secretion of immune stimulatory chemokines or cytokines. Interestingly, another membrane-associated RING ubiquitin ligase, termed Staring, was previously shown to interact with,

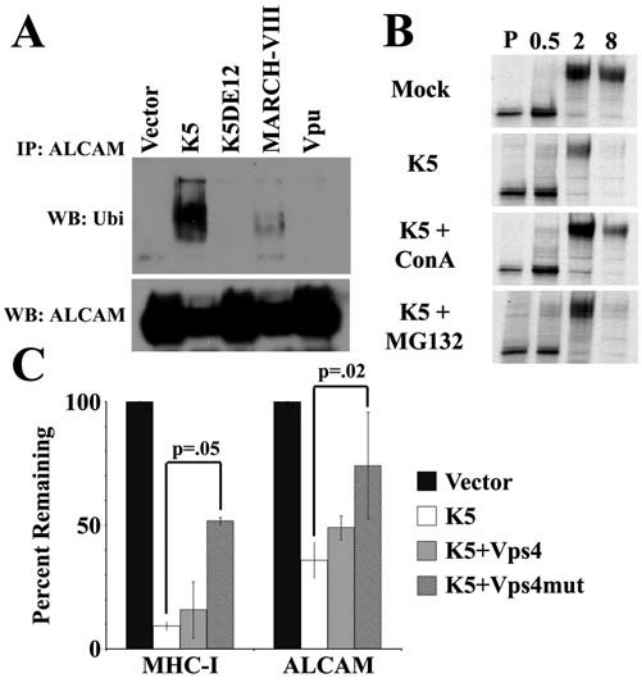

Figure 6. Ubiquitination and Lysosomal Degradation of ALCAM in the Presence of K5

(A) Ubiquitination of ALCAM was examined by co-transfection of HeLa cells with ALCAM-HA as well as the indicated E3 enzymes. Then 24 h post-transfection, cells were lysed in 1% CHAPS, and ALCAM-HA was immunoprecipitated using anti-HA antibody. Samples were resolved on an 8% SDS-PAGE gel, transferred to PVDF, and immunoblotted (WB) with the anti-ubiquitin (Ubi) antibody P4D1 (top) or anti-HA (bottom). Ubiquitinated ALCAM was visible upon co-transfection of K5 and MARCH-VIII, but not with the inactive K5DE12 mutant and the unrelated HIV immune modulator vpu.

(B) To determine whether ubiquitinated ALCAM was degraded by proteasomes or in lysosomes, the fate of newly synthesized ALCAM-HA was determined by metabolic labeling for 10 min with S^{35} Met/Cys and chasing the label for the indicated times (hours) in the presence of the indicated inhibitors. Following lysis, ALCAM-HA was immunoprecipitated using the HA antibody and samples were treated overnight with endoglycosidase H followed by electrophoretic separation. Note the increased recovery of ALCAM at 8 h in the presence of the endosomal/lysosomal proton pump inhibitor concanamycin A (ConA), but not in the presence of the proteasomal inhibitor MG132 (50 μmol).

(C) Surface expression of ALCAM can be restored by overexpressing a dominant negative version of the AAA-ATPase Vps4, which is essential for targeting proteins to MVBs. HeLa cells were transfected as indicated together with GFP to identify transfected cells. Then 24 h post-transfection, cells were harvested and the surface expression of either MHC I or ALCAM was analyzed using flow cytometry. The graph shows the ratio of mean fluorescence intensity from K5-transfected cells to that of control cells after gating for GFP. Data are averaged from three separate experiments.

DOI: 10.1371/journal.ppat.0020107.g006

ubiquitinate, and degrade Syntaxin-1 [56]. It is therefore conceivable that the degradation of Syntaxin-4 by endogenous MARCH proteins plays a role in the turnover of Syntaxin-4, thus regulating exocytosis.

The final novel protein identified by our SILAC screen was ALCAM (CD166). Similar to other proteins downregulated by K5, ALCAM is a type I glycoprotein of the Ig superfamily. Several lines of evidence suggest that ALCAM is a bona fide target of K5. ALCAM downregulation required a functional RING-CH domain and acidic motif in K5. Similar to other K5 target molecules, ALCAM was ubiquitinated and targeted to lysosomes via the MVB pathway. Most likely, K5 ubiquitinates ALCAM at the plasma membrane, resulting in ubiquitin-mediated endocytosis and lysosomal destruction.

In addition, we observed that the myxomavirus protein M153R downregulated ALCAM, likely by a similar mechanism, although this has not been experimentally verified. Previously, it was shown that M153R prevents T cell recognition of myxomavirus-infected cells [13]. In addition, Coscoy and Ganem demonstrated that K5-transfected B cells do not stimulate T cells [21]. While the predominant reason for this lack of T cell recognition is likely the downregulation of MHC I from the cell surface, Coscoy and Ganem showed that the elimination of B7.2 and ICAM-1 further reduces T cell receptor (TCR) signaling [21]. It was thus concluded that the combined effect of preventing both the primary signal via the TCR and the co-stimulatory signals via LFA-1 and CD28, the respective ligands of ICAM-1 and B7.2, minimizes T cell activation by KSHV-infected B cells. Similar to LFA-1 and CD28, ALCAM's ligand, CD6, becomes an integral part of the immunological synapse. Specifically, LFA-1 forms a ring around the synapse, whereas CD28 and CD6 co-localize with the TCR in the center of the synapse [43]. It is generally believed that this supramolecular structure is required for the sustained TCR engagement needed to generate the full repertoire of T cell responses, including signal transduction, cytokine generation, and cell proliferation [57]. Although the function of CD6 has not been studied as extensively as that of LFA-1 and CD28, there is accumulating evidence that the CD6–ALCAM interaction contributes to formation and function of the immunological synapse. It has been shown that antibodies to CD6 activate T cells [58] and that CD6-blocking antibodies or recombinant ALCAM-Fc proteins inhibit T cell proliferation induced by dendritic cells [45]. Taken together, these observations strongly support the notion that, by downregulating ALCAM, K5 and M153R further optimize the ability of their respective viruses to prevent T cell activation. Moreover, the finding that ALCAM is eliminated by immune modulators from both herpesviruses and poxviruses suggests that the ALCAM–CD6 ligand receptor pair plays a previously unappreciated role in antiviral immunity.

In summary, our results validate the use of quantitative proteomics to identify new substrates of viral and cellular immune modulators. In addition to identifying this specific class of transmembrane ubiquitin ligases, it is conceivable that this approach can be used to identify additional targets for any viral proteins that are known to reduce the abundance of their host cell target molecules. Since many viral proteins are thought to be multi-functional, such a systematic, unbiased search for novel host cell targets could help to reveal new functions of viral proteins. This proteomics approach can also be used to find novel targets for cellular proteins that degrade a specific set of targets. In particular, novel substrates for cellular ubiquitin ligases can potentially be found this way. Since ubiquitin ligases are one of the most abundant gene families in the human genome, it is likely that almost every protein in the human genome is regulated by one or more ubiquitin ligases. Identifying the ligase–substrate relationship will be a daunting but important task in unraveling the regulatory networks that govern cellular functions. Novel approaches, as the one described here, are likely to aid this process.

Materials and Methods

Reagents and antibodies. Concanamycin A (Sigma, http://www.sigmaaldrich.com) and MG132 (Sigma) were used at 50 nM and 50 μmol, respectively. The following reagents were obtained as indicated: protein A/G beads (Santa Cruz Biotechnology, http://www.scbt.com), ammonium bicarbonate (Sigma), sodium carbonate (Fisher Scientific, https://www1.fishersci.com), sucrose (Fisher Scientific), and urea (Fisher Scientific). The following antibodies were used: W6/32 (made in-house); anti-BST-2 (GeneTex, http://www.genetex.com); anti-Bap31 (Affinity Bioreagents, http://www.bioreagents.com); anti-Syntaxin-4, anti-CD9, and anti-ALCAM (BD Biosciences, http://www.bdbiosciences.com); anti-Flag:FitC and anti-HA (Sigma); anti-ubiquitin (clone P4D1 from Invitrogen, http://www.invitrogen.com); anti-CD29 (University of Iowa Developmental Studies Hybridoma Bank, http://www.uiowa.edu/~dshbwww); and goat anti-mouse Alexa Fluor 594 (Molecular Probes, http://probes.invitrogen.com).

Plasmids and cloning. The following plasmids have been described previously: K5 C-Flag/pUHD10–1, K5 RING C-Flag/pUDH10–1, K3/pUDH10–1, M153R C-Flag/pUHD10–1, K5DE12 C-Flag/pUHD10–1, plasmids expressing both Vps4 and Vps4mut, and all full-length MARCH constructs in pUHD10–1 [12,14,38,59]. An adenoviral vector expressing K5 C-Flag (Ad-K5) has been described previously [19]. Adenovirus-expressing vpu was a generous gift from A. Moses (Vaccine and Gene Therapy Institute, United States).

A plasmid containing the ALCAM cDNA was a gift from G. Swart (Radboud University, Netherlands). ALCAM-HA was generated from this plasmid by PCR amplification of the ALCAM open reading frame. A C-terminal HA tag was added during the amplification. The PCR product was then digested using suitable enzymes and ligated into the pUHD10–1 vector. MARCH-VIII truncation mutants (Δ46, Δ62, and Δ74) were generated by PCR amplification of the given region. An N-terminal FLAG tag was added to each construct during amplification. Each PCR was then digested using suitable enzymes and ligated into the mammalian-expressing vector pUHD10–1. An adenoviral vector expressing MARCH-VIII was generated by cloning the full-length open reading frame from MARCH-VIII into the pShuttle vector (Stratagene, http://www.stratagene.com). Ad-MARCH-VIII virus was generated by linearization, transfection, and amplification according to the manufacturer's directions.

Culture conditions. Prior to labeling, HeLa-Tet Off cells were grown in DMEM (Invitrogen) supplemented with 10% fetal calf serum (Hyclone, http://www.hyclone.com) and 1× Pen/Strep (Invitrogen). KSHV-infected DMVECs were established and maintained as previously described [47]. KSHV-infected DMVECs were used in experiments when >90% of the cells expressed LANA-1.

Stable isotope labeling of HeLa cells. Cells were labeled with stable isotopes using labeling medium (DMEM, Invitrogen) lacking the amino acids L-lysine and L-leucine (prepared according to the manufacturer's protocol). Medium was supplemented with 10% dialyzed fetal calf serum (Hyclone), 1× Pen/Strep (Invitrogen), and either isotopically light L-lysine and L-leucine (Sigma) or isotopically heavy L-lysine (U-13C6, 98%; U-15N2, 98%) and L-leucine (U-13C6, 98%; 15N, 98%) (Cambridge Isotope, http://www.isotope.com). Cells were maintained in labeling medium for 6 d prior to initiation of the experiment to insure complete labeling.

Preparation of samples for MS/MS analysis. Cells grown in labeling medium were infected with either Ad-K5 (heavy-labeled cells) or Ad-WT (light-labeled cells) at an MOI of 25. Then 24 h post-infection, cells were harvested by scraping, washed twice in PBS, resuspended in PBS containing 5 mM EDTA, and lysed by douncing. Unlysed cells and debris were cleared from the lysate by centrifugation for 5 min at 3,000 × *g*. The cleared lysates were separated into membrane and soluble fractions by centrifugation for 30 min at 45,000 × *g*. The membrane fraction was resuspended in PBS by sonication and separated over a discontinous sucrose gradient (2 M, 1.6 M, 1.25 M, 1.2 M, and 0.8 M) by centrifugation for 2.5 h at 25,000 rpm (Sorvall SW-28 rotor, http://www.sorvall.com). The bands corresponding to the plasma membrane (0.8–1.2 M interphase), Golgi (1.25–1.2 M interphase), and ER (1.6–1.25 M interphase) fractions were removed, diluted 5× in Tris-EDTA (pH 8.0), and centrifuged for 30 min at 45,000 × *g* to pellet the proteins contained in each fraction. Pellets were washed for 30 min in 50 mM sodium bicarbonate (pH 11.5) and centrifuged for 30 min at 45,000 × *g*, followed by a second wash in 50 mM ammonium bicarbonate (pH 8.5) and further centrifugation for 30 min at 45,000 × *g*. Final pellets were resuspended in 8.0 M deionized urea and 50 mM ammonium bicarbonate (pH 8.5) and protein levels quantitated using the Bio-Rad Protein Assay (Bio-Rad, http://www.biorad.com). Samples were reduced with DTT (Sigma) and alkylated with iodoacetamide (Sigma) prior to overnight digestion with trypsin (Promega, http://www.promega.com).

Chromatography, MS, and informatics. Peptide mixtures were analyzed by electrospray ionization tandem MS, coupled to two-dimensional liquid chromatography, which was performed using a modified version of the protocol described by Link and coworkers [60]. Briefly, 22 μg of sample was loaded onto an Opti-Pak capillary SCX trap cartridge (Optimize Technologies, http://www.optimizetech.com) and eluted stepwise (12.5, 25, 37.5, 50, 62.5, 75, 87.5, 100, 112.5, 125, 200, 300, or 450 mM ammonium acetate in 0.1% formic acid) onto a reverse phase C-18 capillary column (180 μm × 100 mm, BioBasic-18; Thermo Electron, http://www.thermo.com). Peptides were then eluted using an acetonitrile gradient (5%, 5 min; 5%–40%, 75 min; 40%–90%, 10 min) into a ProteomeX LCQ Deca XP Plus mass spectrometer (Thermo Electron) equipped with a low-flow (1 μl/min) electrospray source. The instrument was set to trigger data-dependent MS/MS acquisition of the three most intense ions detected during the MS survey scan when total ion current per MS survey scan exceeded 5.0×10^5 counts.

Proteins were identified by analyzing tandem mass spectra with the Sequest algorithm (Thermo Electron) as described by Yates et al. [61] using the human subset of the UniProt/Swiss-Prot protein database (UniProt release 5.1, http://www.expasy.org/sprot). The search results were further analyzed using PeptideProphet [32]. SILAC ratios were determined using the ASAPRatio algorithm [34]. Multiple peptides derived from a single protein were included if PeptideProphet probability was greater than or equal to 0.85. All positive results were manually verified. The putative subcellular localization of proteins was determined using the Swiss-Prot database.

Immune fluorescence and flow cytometry. Cells (1.5×10^4) were plated on 15-mm coverslips (Fisher Scientific) and allowed to adhere overnight prior to transfection. Following transfection, cells were washed with PBS, fixed with 2% paraformaldehyde for 20 min at room temperature, and permeabilized with 0.2% Triton X-100 for 3 min at room temperature. Nonspecific binding sites were blocked with 3% BSA and 0.5% fish gelatin in PBS for 30 min at 37 °C. The fixed cells were incubated overnight at 37 °C with primary antibody diluted in blocking solution. Secondary and conjugated antibodies were diluted in blocking solution and incubated with the cells for at least 30 min at 37 °C. Cells were washed six times with PBS between all antibody treatments. Slides were fixed a second time in 2% paraformaldehyde after the final antibody treatment and washed twice with PBS. Coverslips were then mounted on slides and covered with Vectashield H-1200 + DAPI (Vector Laboratories, http://www.vectorlabs.com).

For flow cytometry, cells were removed from tissue culture dishes with 0.05% trypsin-EDTA (Invitrogen), washed with ice-cold PBS, and incubated with appropriate antibody for 30 min at 4 °C. The cells were washed with ice-cold PBS and either resuspended in ice-cold PBS or incubated with PE-conjugated anti-mouse secondary antibody (Dako, http://www.dako.com) and washed again before analysis with a BD Biosciences FACSCalibur flow cytometer.

Metabolic labeling, immunoprecipitation, and Western blotting. HeLa cells were grown to 80% confluency in 100-mm tissue culture dishes and were transfected as above. At 24 h post-infection, cells were incubated in serum-free and methionine-free medium for 30 min, and metabolically labeled with ^{35}S-cysteine/^{35}S-methionine (300 μCi/plate; Amersham, http://www.amersham.com) for 20 min. After labeling, cells were washed twice with PBS and the label was chased for the indicated time in DMEM containing excess cold methionine/cysteine. Following chase, cells were lysed in PBS containing 1% NP-40 and protease inhibitors (Roche, http://www.roche.com). The cell lysate was pre-cleared with protein A/G agarose beads overnight and incubated with 3 μg of antibody for 1 h, followed by 1 h with protein A/G beads. Immunoprecipated proteins were washed five times with 1% NP-40 in PBS. All samples were boiled in Laemmli buffer and analyzed by SDS-PAGE gel electrophoresis. Gels were fixed, dried, and exposed to Kodak (http://www.kodak.com) BioMax MR film. Western blotting was accomplished using the Western-Breeze Chemiluminescent Detection System (Invitrogen) following semi-dry transfer to PVDF membranes (Millipore, http:// www.millipore.com).

Supporting Information

Accession Numbers

The UniGene (http://www.ncbi.nlm.nih.gov/entrez/query.fcgi?db=unigene) accession numbers for ALCAM, BST-2, and Syntaxin-4 are Hs.591293, Hs.118110, and Hs.83734, respectively.

Acknowledgments

We would like to thank members of the Früh lab, particularly Mandana Mansouri and Kristine Gouveia, for reagents and Kasinath Viswanathan for help with the mass spectrometric analysis. We thank Kristine Alexander for constructing the MARCH-VIII truncation mutants. We further thank Guido Swart, University of Nijmegen, for the ALCAM construct, and Robert Means and Sabine Lang, Yale University, for unpublished information.

Author contributions. KF conceived and designed the experiments. EB performed the experiments. AM maintained and ran the mass spectroscope and analyzed the data. EB and KF wrote the paper.

Funding. This work was supported by RO1 CA/AI 09401 and R21 CA 109674–02 to KF. EB was supported by Ruth L. Kirschstein National Research Service Award T32AI007472 and a Tartar fellowship.

Competing interests. The authors have declared that no competing interests exist.

References

1. Wiertz EJ, Jones TR, Sun L, Bogyo M, Geuze HJ, et al. (1996) The human cytomegalovirus US11 gene product dislocates MHC class I heavy chains from the endoplasmic reticulum to the cytosol. Cell 84: 769–779.
2. Johnson DC, Hegde NR (2002) Inhibition of the MHC class II antigen presentation pathway by human cytomegalovirus. Curr Top Microbiol Immunol 269: 101–115.
3. Ziegler H, Muranyi W, Burgert HG, Kremmer E, Koszinowski UH (2000) The luminal part of the murine cytomegalovirus glycoprotein gp40 catalyzes the retention of MHC class I molecules. EMBO J 19: 870–881.
4. Lodoen M, Ogasawara K, Hamerman JA, Arase H, Houchins JP, et al. (2003) NKG2D-mediated natural killer cell protection against cytomegalovirus is impaired by viral gp40 modulation of retinoic acid early inducible 1 gene molecules. J Exp Med 197: 1245–1253.
5. Kerkau T, Bacik I, Bennink JR, Yewdell JW, Hunig T, et al. (1997) The human immunodeficiency virus type 1 (HIV-1) Vpu protein interferes with an early step in the biosynthesis of major histocompatibility complex (MHC) class I molecules. J Exp Med 185: 1295–1305.
6. Willey RL, Maldarelli F, Martin MA, Strebel K (1992) Human immunodeficiency virus type 1 Vpu protein induces rapid degradation of CD4. J Virol 66: 7193–7200.
7. Garcia JV, Miller AD (1992) Downregulation of cell surface CD4 by nef. Res Virol 143: 52–55.
8. Collins KL, Chen BK, Kalams SA, Walker BD, Baltimore D (1998) HIV-1 Nef protein protects infected primary cells against killing by cytotoxic T lymphocytes. Nature 391: 397–401.
9. Coscoy L, Ganem D (2000) Kaposi's sarcoma-associated herpesvirus encodes two proteins that block cell surface display of MHC class I chains by enhancing their endocytosis. Proc Natl Acad Sci U S A 97: 8051–8056.
10. Ishido S, Wang C, Lee BS, Cohen GB, Jung JU (2000) Downregulation of major histocompatibility complex class I molecules by Kaposi's sarcoma-associated herpesvirus K3 and K5 proteins. J Virol 74: 5300–5309.
11. Sanchez DJ, Coscoy L, Ganem D (2002) Functional organization of MIR2, a novel viral regulator of selective endocytosis. J Biol Chem 277: 6124–6130.
12. Mansouri M, Bartee E, Gouveia K, Hovey Nerenberg BT, Barrett J, et al. (2003) The PHD/LAP-domain protein M153R of myxomavirus is a ubiquitin ligase that induces the rapid internalization and lysosomal destruction of CD4. J Virol 77: 1427–1440.
13. Guerin JL, Gelfi J, Boullier S, Delverdier M, Bellanger FA, et al. (2002) Myxoma virus leukemia-associated protein is responsible for major histocompatibility complex class I and Fas-CD95 down-regulation and defines scrapins, a new group of surface cellular receptor abductor proteins. J Virol 76: 2912–2923.
14. Bartee E, Mansouri M, Hovey Nerenberg BT, Gouveia K, Fruh K (2004) Downregulation of major histocompatibility complex class I by human ubiquitin ligases related to viral immune evasion proteins. J Virol 78: 1109–1120.
15. Goto E, Ishido S, Sato Y, Ohgimoto S, Ohgimoto K, et al. (2003) c-MIR, a human E3 ubiquitin ligase, is a functional homolog of herpesvirus proteins MIR1 and MIR2 and has similar activity. J Biol Chem 278: 14657–14668.
16. Boname JM, Stevenson PG (2001) MHC class I ubiquitination by a viral PHD/LAP finger protein. Immunity 15: 627–636.
17. Coscoy L, Sanchez DJ, Ganem D (2001) A novel class of herpesvirus-encoded membrane-bound E3 ubiquitin ligases regulates endocytosis of proteins involved in immune recognition. J Cell Biol 155: 1265–1273.
18. Hewitt EW, Duncan L, Mufti D, Baker J, Stevenson PG, et al. (2002) Ubiquitylation of MHC class I by the K3 viral protein signals internalization and TSG101-dependent degradation. EMBO J 21: 2418–2429.
19. Mansouri M, Douglas J, Rose PP, Gouveia K, Thomas G, et al. (2006) Kaposi's sarcoma herpesvirus K5 eliminates CD31/PECAM from endothelial cells. Blood 108: 1932–1940.
20. Sanchez DJ, Gumperz JE, Ganem D (2005) Regulation of CD1d expression and function by a herpesvirus infection. J Clin Invest 115: 1369–1378.
21. Coscoy L, Ganem D (2001) A viral protein that selectively downregulates ICAM-1 and B7–2 and modulates T cell costimulation. J Clin Invest 107: 1599–1606.
22. Ishido S, Choi JK, Lee BS, Wang C, DeMaria M, et al. (2000) Inhibition of natural killer cell-mediated cytotoxicity by Kaposi's sarcoma-associated herpesvirus K5 protein. Immunity 13: 365–374.
23. Joazeiro CA, Weissman AM (2000) RING finger proteins: Mediators of ubiquitin ligase activity. Cell 102: 549–552.
24. Ong SE, Mann M (2005) Mass spectrometry-based proteomics turns quantitative. Nat Chem Biol 1: 252–262.
25. Ong SE, Blagoev B, Kratchmarova I, Kristensen DB, Steen H, et al. (2002) Stable isotope labeling by amino acids in cell culture, SILAC, as a simple and accurate approach to expression proteomics. Mol Cell Proteomics 1: 376–386.
26. Ong SE, Foster LJ, Mann M (2003) Mass spectrometric-based approaches in quantitative proteomics. Methods 29: 124–130.
27. Everley PA, Krijgsveld J, Zetter BR, Gygi SP (2004) Quantitative cancer proteomics: Stable isotope labeling with amino acids in cell culture (SILAC) as a tool for prostate cancer research. Mol Cell Proteomics 3: 729–735.
28. Kolkman A, Slijper M, Heck AJ (2005) Development and application of proteomics technologies in *Saccharomyces cerevisiae*. Trends Biotechnol 23: 598–604.
29. Gruhler A, Schulze WX, Matthiesen R, Mann M, Jensen ON (2005) Stable isotope labeling of *Arabidopsis thaliana* cells and quantitative proteomics by mass spectrometry. Mol Cell Proteomics 4: 1697–1709.
30. Lehner PJ, Hoer S, Dodd R, Duncan LM (2005) Downregulation of cell surface receptors by the K3 family of viral and cellular ubiquitin E3 ligases. Immunol Rev 207: 112–125.
31. Yates JR 3rd, Eng JK, McCormack AL (1995) Mining genomes: Correlating tandem mass spectra of modified and unmodified peptides to sequences in nucleotide databases. Anal Chem 67: 3202–3210.
32. Keller A, Nesvizhskii AI, Kolker E, Aebersold R (2002) Empirical statistical model to estimate the accuracy of peptide identifications made by MS/MS and database search. Anal Chem 74: 5383–5392.
33. Durr E, Yu J, Krasinska KM, Carver LA, Yates JR, et al. (2004) Direct proteomic mapping of the lung microvascular endothelial cell surface in vivo and in cell culture. Nat Biotechnol 22: 985–992.
34. Li XJ, Zhang H, Ranish JA, Aebersold R (2003) Automated statistical analysis of protein abundance ratios from data generated by stable-isotope dilution and tandem mass spectrometry. Anal Chem 75: 6648–6657.
35. Ishikawa J, Kaisho T, Tomizawa H, Lee BO, Kobune Y, et al. (1995) Molecular cloning and chromosomal mapping of a bone marrow stromal cell surface gene, BST2, that may be involved in pre-B-cell growth. Genomics 26: 527–534.
36. Ohtomo T, Sugamata Y, Ozaki Y, Ono K, Yoshimura Y, et al. (1999) Molecular cloning and characterization of a surface antigen preferentially overexpressed on multiple myeloma cells. Biochem Biophys Res Commun 258: 583–591.
37. Kupzig S, Korolchuk V, Rollason R, Sugden A, Wilde A, et al. (2003) Bst-2/HM1.24 is a raft-associated apical membrane protein with an unusual topology. Traffic 4: 694–709.
38. Paulson E, Tran C, Collins C, Früh K (2001) KSHV-K5 inhibits phosphorylation of the major histocompatibility complax class I tail. Virology 288: 369–378.
39. Salaun C, James DJ, Greaves J, Chamberlain LH (2004) Plasma membrane targeting of exocytic SNARE proteins. Biochim Biophys Acta 1693: 81–89.
40. Fukuda H, Nakamura N, Hirose S (2006) MARCH-III is a novel component of endosomes with properties similar to those of MARCH-II. J Biochem (Tokyo) 139: 137–145.
41. Nakamura N, Fukuda H, Kato A, Hirose S (2005) MARCH-II is a syntaxin-6-binding protein involved in endosomal trafficking. Mol Biol Cell 16: 1696–1710.
42. Bowen MA, Bajorath J, D'Egidio M, Whitney GS, Palmer D, et al. (1997) Characterization of mouse ALCAM (CD166): The CD6-binding domain is conserved in different homologs and mediates cross-species binding. Eur J Immunol 27: 1469–1478.
43. Gimferrer I, Calvo M, Mittelbrunn M, Farnos M, Sarrias MR, et al. (2004) Relevance of CD6-mediated interactions in T cell activation and proliferation. J Immunol 173: 2262–2270.
44. Hassan NJ, Barclay AN, Brown MH (2004) Frontline: Optimal T cell activation requires the engagement of CD6 and CD166. Eur J Immunol 34: 930–940.
45. Zimmerman AW, Joosten B, Torensma R, Parnes JR, van Leeuwen FN, et al. (2006) Long-term engagement of CD6 and ALCAM is essential for T-cell proliferation induced by dendritic cells. Blood 107: 3212–3220.
46. Means RE, Ishido S, Alvarez X, Jung JU (2002) Multiple endocytic trafficking pathways of MHC class I molecules induced by a herpesvirus protein. EMBO J 21: 1638–1649.
47. Moses AV, Fish KN, Ruhl R, Smith PP, Strussenberg JG, et al. (1999) Long-term infection and transformation of dermal microvascular endothelial cells by human herpesvirus 8. J Virol 73: 6892–6902.
48. Garrus JE, von Schwedler UK, Pornillos OW, Morham SG, Zavitz KH, et al.

(2001) Tsg101 and the vacuolar protein sorting pathway are essential for HIV-1 budding. Cell 107: 55–65.
49. Loyet KM, Ouyang W, Eaton DL, Stults JT (2005) Proteomic profiling of surface proteins on Th1 and Th2 cells. J Proteome Res 4: 400–409.
50. Gronborg M, Kristiansen TZ, Iwahori A, Chang R, Reddy R, et al. (2006) Biomarker discovery from pancreatic cancer secretome using a differential proteomic approach. Mol Cell Proteomics 5: 157–171.
51. Blagoev B, Kratchmarova I, Ong SE, Nielsen M, Foster LJ, et al. (2003) A proteomics strategy to elucidate functional protein-protein interactions applied to EGF signaling. Nat Biotechnol 21: 315–318.
52. Neher SB, Villen J, Oakes EC, Bakalarski CE, Sauer RT, et al. (2006) Proteomic profiling of ClpXP substrates after DNA damage reveals extensive instability within SOS regulon. Mol Cell 22: 193–204.
53. Hitchcock AL, Auld K, Gygi SP, Silver PA (2003) A subset of membrane-associated proteins is ubiquitinated in response to mutations in the endoplasmic reticulum degradation machinery. Proc Natl Acad Sci U S A 100: 12735–12740.
54. Peng J, Schwartz D, Elias JE, Thoreen CC, Cheng D, et al. (2003) A proteomics approach to understanding protein ubiquitination. Nat Biotechnol 21: 921–926.
55. Saito T, Okada S, Yamada E, Ohshima K, Shimizu H, et al. (2003) Syntaxin 4 and Synip (syntaxin 4 interacting protein) regulate insulin secretion in the pancreatic beta HC-9 cell. J Biol Chem 278: 36718–36725.
56. Chin LS, Vavalle JP, Li L (2002) Staring, a novel E3 ubiquitin-protein ligase that targets syntaxin 1 for degradation. J Biol Chem 277: 35071–35079.
57. Lin J, Miller MJ, Shaw AS (2005) The c-SMAC: Sorting it all out (or in). J Cell Biol 170: 177–182.
58. Gangemi RM, Swack JA, Gaviria DM, Romain PL (1989) Anti-T12, an anti-CD6 monoclonal antibody, can activate human T lymphocytes. J Immunol 143: 2439–2447.
59. Bishop N, Woodman P (2000) ATPase-defective mammalian VPS4 localizes to aberrant endosomes and impairs cholesterol trafficking. Mol Biol Cell 11: 227–239.
60. Link AJ, Eng J, Schieltz DM, Carmack E, Mize GJ, et al. (1999) Direct analysis of protein complexes using mass spectrometry. Nat Biotechnol 17: 676–682.
61. Yates JR 3rd, Eng JK, McCormack AL, Schieltz D (1995) Method to correlate tandem mass spectra of modified peptides to amino acid sequences in the protein database. Anal Chem 67: 1426–1436.